

Source modeling of hypothetical Tokai-Tonankai-Nankai, Japan, earthquake and strong ground motion simulation using the empirical Green's functions



Y. Ishii & K. Dan

Ohsaki Research Institute, Inc., Tokyo

H. Takahashi

Oyo Corporation, Nagoya

J. Miyakoshi, M. Mori, & N. Fukuwa

Nagoya University, Nagoya

SUMMARY:

The fault rupturing has been modeled differently and separately for the strong ground motions and tsunami because of the differences of the analysis methods and the focussed periods, although both of the strong ground motions and tsunami are the results of the common fault rupturing. We proposed a procedure for making a consistent source model both for the strong ground motions and tsunami, and applied our new procedure to the huge subduction earthquake (M_w 9.1) along the Nankai Trough, and showed two examples of the fault models including some asperities. We simulated strong ground motions using the empirical Green's functions in and around Aichi Prefecture. And the JMA seismic intensities of the synthetic waveforms in case that the short-period level was assumed to be equal to the average for crustal earthquakes were comparable to those in the 1854 Ansei-Tokai earthquake.

Keywords: Nankai Trough, Tokai-Tonankai-Nankai earthquake, source process, strong ground motion

1. INTRODUCTION

The 2011 off the Pacific coast of Tohoku, Japan, earthquake (M_w 9.0) occurred on March 11. Since the magnitude of this earthquake was much larger than expected, the Central Disaster Management Council of Japan has re-evaluated the earthquake size along the Nankai Trough (Fig.1.1). This focal area has a shallower part of the fault that increases tsunami as well as a deeper part of the fault that causes strong ground motions and tsunami. Meanwhile, the fault rupturing has been modeled differently and separately for the strong ground motions and tsunami because of the differences of the analysis methods and the focussed periods. Hence, in this paper, we propose a consistent source model both for the strong ground motions and tsunami of the huge subduction earthquake along the Nankai Trough. And we simulate strong ground motions in and around Aichi Prefecture using the empirical Green's functions based on the fault models including some asperities.

2. SOURCE MODELING

2.1. Fault Parameters

The focal area along the Nankai Trough in Fig. 1.1 shows that a deeper part of the fault area which causes strong ground motions and tsunami is about 110 thousand km^2 and that a shallower part of the fault area which increases tsunami is about 30 thousand km^2 . Therefore, the total fault area is 140 thousand km^2 . The fault length is about 750 km, then the fault width is 186 km on average. The flow of setting parameters is shown in Fig. 2.1. We set parameters based on the flow in Fig. 2.1.

In Fig. 2.1, at first, the moment magnitude M_w and the seismic moment M_0 are given by the equations below (Utsu, 2001):

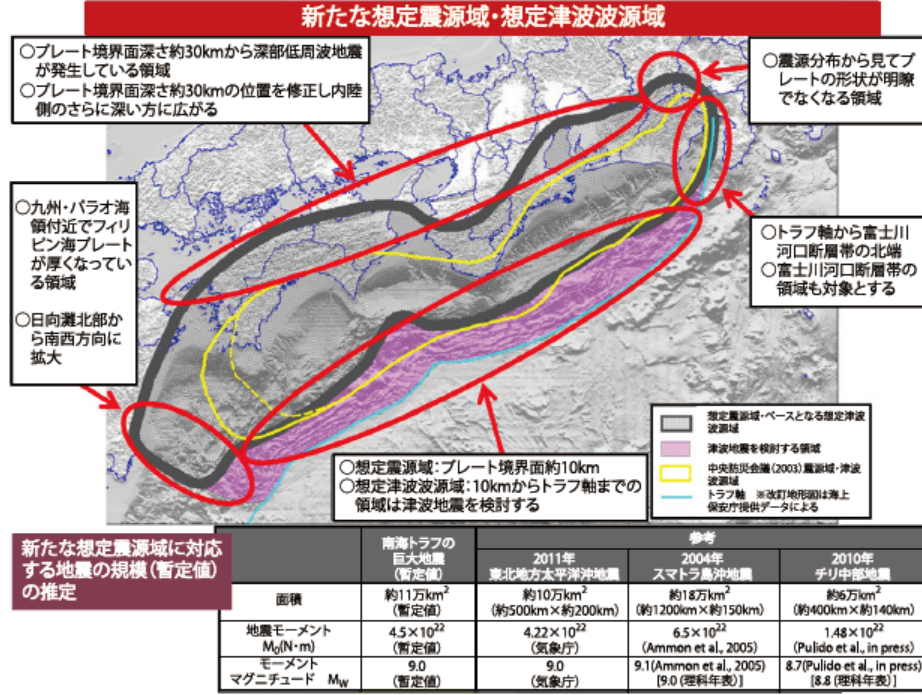


Figure 1.1. Focal area for the huge earthquake along the Nankai Trough (Central Disaster Management Council, 2012).

$$M_w = \log S[\text{km}^2] + 4.0, \quad (2.1)$$

$$M_0[\text{dyne} \cdot \text{cm}] = 10^{1.5M_w + 16.1}. \quad (2.2)$$

The stress drop $\Delta\sigma$ is given by the following equation (Eshelby, 1957):

$$\Delta\sigma = (7/16)M_0(S/\pi)^{1.5}. \quad (2.3)$$

Here, S is the fault area. The stress drop $\Delta\sigma$ is calculated to be 30.7 bars from Eqn. 2.1 to Eqn. 2.3.

The short-period level A of the 2011 off the Pacific coast of Tohoku earthquake was twice the average value to the seismic moment proposed by Dan *et al.* (2001) for crustal earthquakes. We assumed the short-period level to be the average to the seismic moment for crustal earthquakes in Case 1 and twice the average in Case 2 as follows:

$$A[\text{dyne} \cdot \text{cm}/\text{s}^2] = 2.46 \times 10^{17} \times M_0[\text{dyne} \cdot \text{cm}/\text{s}^2]^{1/3} \times (1 \text{ or } 2). \quad (2.4)$$

The stress drop $\Delta\sigma$ and the short-period level A are related with other parameters as follows:

$$\Delta\sigma = (S_{asp}/S)\Delta\sigma_{asp}, \quad (2.5)$$

$$A = 4\pi\beta_{deep}^2(S_{asp}/\pi)^{1/2}\Delta\sigma_{asp}. \quad (2.6)$$

Here, S_{asp} is the area of the asperities, $\Delta\sigma_{asp}$ is the stress drop on the asperities, and β_{deep} is the S -wave velocity of the deeper part. The stress drop on the asperities $\Delta\sigma_{asp}$ and the area of the asperities S_{asp} can be calculated by the following equations from Eqn. 2.5 and Eqn. 2.6:

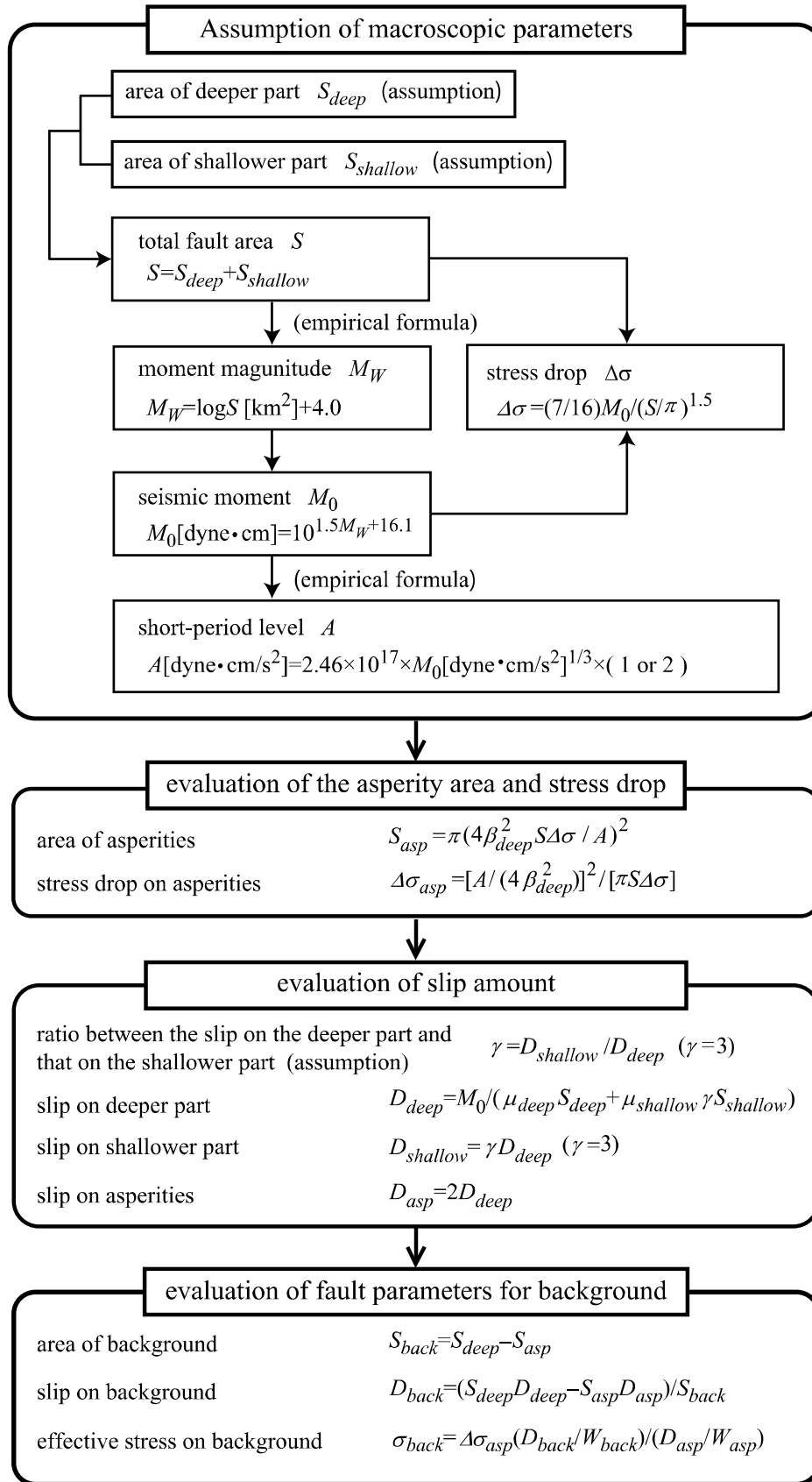


Figure 2.1. Flow of setting fault parameters

$$S_{asp} = \pi(4\beta_{deep}^2 S \Delta\sigma / A)^2, \quad (2.7)$$

$$\Delta\sigma_{asp} = [A / (4\beta_{deep}^2)]^2 / [\pi S \Delta\sigma]. \quad (2.8)$$

The seismic moment M_0 is expressed as follows:

$$M_0 = \mu_{deep} S_{deep} D_{deep} + \mu_{shallow} S_{shallow} D_{shallow}. \quad (2.9)$$

Here, μ_{deep} is the shear rigidity of the deeper part, D_{deep} is the slip on the deeper part, $\mu_{shallow}$ is the shear rigidity of the shallower part, and $D_{shallow}$ is the slip on the shallower part.

The ratio γ between the slip on the deeper part and that on the shallower part is assumed to be 3, because the ratio was about 3 in the 2011 off the Pacific coast of Tohoku earthquake (Yoshida *et al.*, 2011).

$$D_{shallow} = \gamma D_{deep} \quad (\gamma = 3). \quad (2.10)$$

The slip on the deeper part D_{deep} can be calculated by the following equations from Eqn. 2.9 and Eqn. 2.10.

$$D_{deep} = M_0 / (\mu_{shallow} \gamma S_{shallow} + \mu_{deep} S_{deep}). \quad (2.11)$$

The slip on the asperities D_{asp} can be set based on Somerville *et al.* (1999) as follows:

$$D_{asp} = 2D_{deep}. \quad (2.12)$$

The area, the seismic moment, and the slip on the background are related with other parameters as follows:

$$S_{back} = S_{deep} - S_{asp}, \quad (2.13)$$

$$M_{0deep} = M_{0asp} + M_{0back}, \quad (2.14)$$

$$D_{back} = (S_{deep} D_{deep} - S_{asp} D_{asp}) / S_{back}. \quad (2.15)$$

The fault parameters of the huge earthquake along the Nankai Trough are shown in Table 2.1. The locations of the asperities and the hypocenter are based on the fault model of the subduction earthquake along the Nankai Trough proposed by the Central Disaster Management Council (2003). The fault models of the huge earthquake along the Nankai Trough for predicting strong ground motions and tsunami is shown in Fig. 2.2. The depth of the plate boundary was assumed according to the crustal structure provided by Japan Agency for Marine-earth Science and Technology.

3. SYNTHESIS

3.1. Strong Ground Motion Data

We used observed strong ground motions at 4 stations (NGY, AICP12, SZO024, and MIEP02) in and around Aichi Prefecture as empirical Green's functions during 4 small events near the source area. NGY is the station of Nagoya City, AICP12 is the station of Aichi Prefecture, SZO024 is the station of K-NET, and MIEP02 is the station of Mie Prefecture. Figure 3.1 shows the locations of these stations together with the epicenters and the focal mechanisms of the small events. Table 3.1 lists the fault parameters of the small events used as the empirical Green's functions. Figure 3.2 shows the observed waveforms of the small events at NGY.

Table 2.1. Fault parameters of the huge earthquake along the Nankai Trough

area of deeper part	area of shallower part	total fault area	moment magnitude	seismic moment	stress drop		
S_{deep}	$S_{shallow}$	S	MW	M_0	$\Delta\sigma$		
[km ²]	[km ²]	[km ²]		[dyne · cm]	[bar]		
110×10^3	30×10^3	140×10^3	9.1	6.59×10^{29}	30.7		
short-period level	area of asperities	stress drop on asperities	slip on deeper part	slip on asperities	slip on background	slip on shallower part	effective stress on background
A	S_{asp}	$\Delta\sigma_{asp}$	D_{deep}	D_{asp}	D_{back}	$D_{shallow}$	σ_{back}
[dyne · cm/s ²]	[km ²]	[bar]	[m]	[m]	[m]	[m]	[bar]
Case 1: the short-period level is assumed to be equal to the average for crustal earthquakes							
2.14×10^{27}	43000	100	10	20	3.6	30	11
Case 2: the short-period level is assumed to be twice the average for crustal earthquakes							
4.28×10^{27}	10800	400	10	20	8.9	30	56

$\gamma = D_{shallow}/D_{deep} = 3$, $\mu_{shallow} = 2.34 \times 10^{11}$ dyne/cm², $\beta_{shallow} = 3.00$ km/s, $\mu_{deep} = 4.10 \times 10^{11}$ dyne/cm², and $\beta_{deep} = 3.82$ km/s.

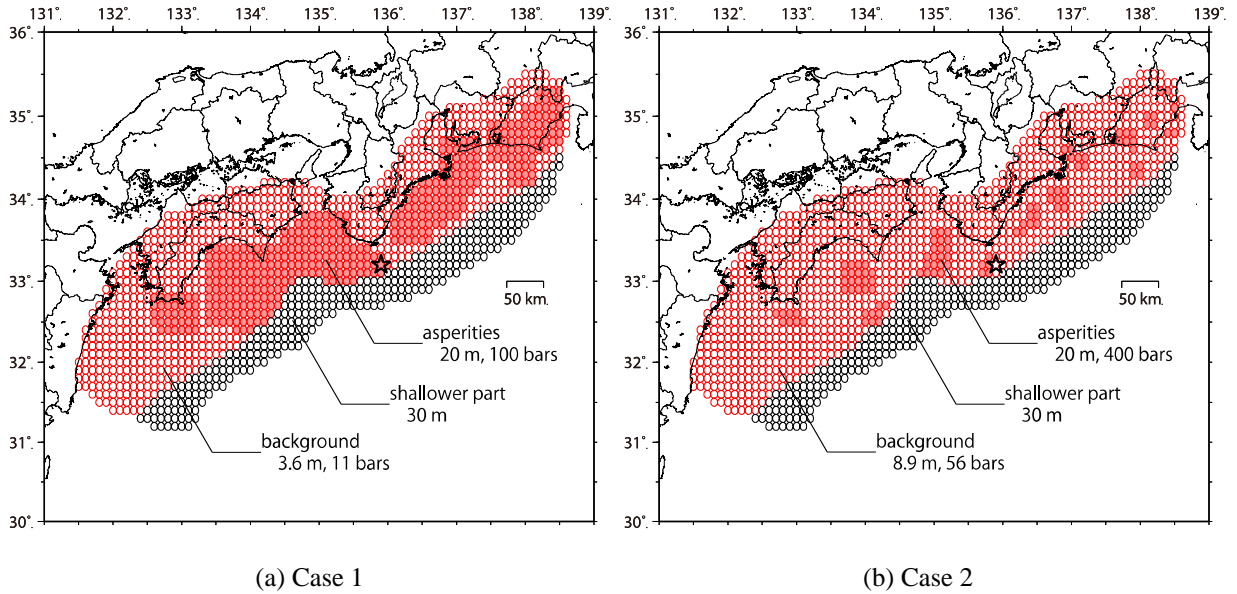


Figure 2.2. Fault models of the huge earthquake along the Nankai Trough for predicting strong ground motion and tsunami. The star is the hypocenter. The black sub-faults are the shallower part which increases tsunami. Others are the deeper part, and the red shaded sub-faults are the asperities.

We assigned ground motion records of the small event to the nearest sub-faults.

3.2 Results

Figure 3.3 shows the synthetic waveforms, and Fig. 3.4 shows the pseudo velocity response spectra of the synthetic waveforms. The thin dashed line in Fig. 3.4 is the level 2 spectra by Japanese government notification, which is the design response spectrum in Japan, and the return period of which is more than 500 years. The pseudo velocity response spectra of Case 1 are larger than the level 2 spectra in the period range larger than about 1 sec.

The pseudo velocity response spectrum of Case 2 are about twice as large as those of Case 1 in the entire period range. This is because the short-period level in Case 1 is twice larger than that in Case 2. Table 3.2 summarizes the instrumental seismic intensities and the JMA seismic intensities of the

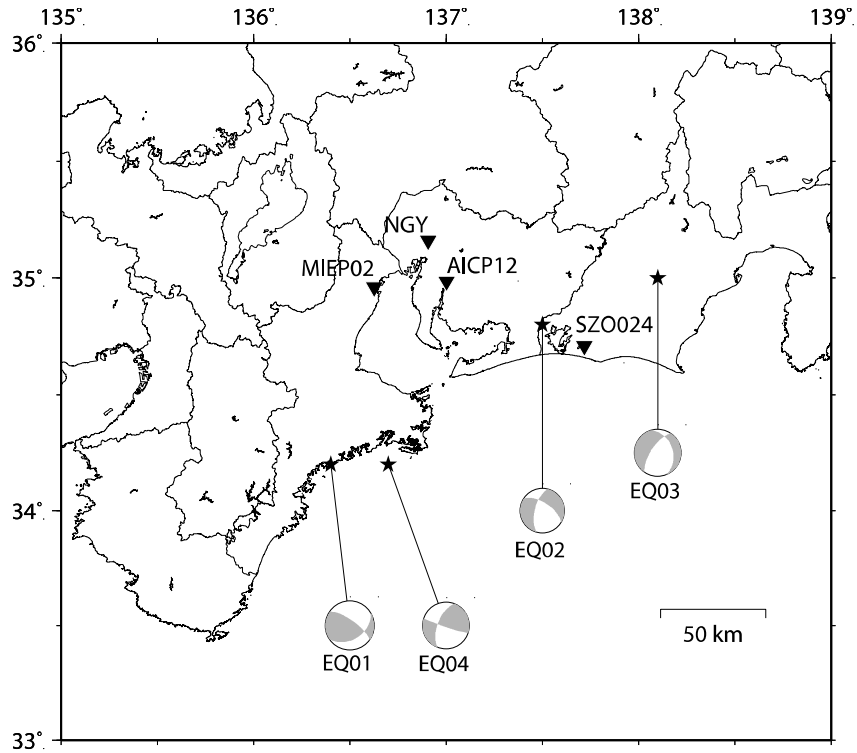


Figure 3.1. Locations of the sites and the epicenters and the focal mechanisms of the events for the empirical Green's functions.

Table 3.1. Fault parameter of the empirical Green's functions

No.	date	moment magnitude M_W	latitude	longitude	depth [km]	seismic moment M_0 [dyne · cm]	slip D [m]	fault area S [km ²]	stress drop $\Delta\sigma$ [bar]	short period level A [dyne · cm/s ²]
EQ01	2000.10.31	5.4	34.2 N	136.4 E	38.0	1.70E+24	0.59	4.65	413	1.23E+26
EQ02	2001.02.23	4.9	34.8 N	137.5 E	32.0	2.43E+23	0.39	0.99	600	8.24E+25
EQ03	2001.04.03	5.2	35.0 N	138.1 E	35.0	8.17E+23	0.3	4.32	222	6.36E+25
EQ04	2004.01.06	5.2	34.2 N	136.7 E	40.0	6.74E+23	0.17	6.46	100	3.51E+25

$\rho=3.2 \text{ g/cm}^3$, $\beta=4.41 \text{ km/s}$, and $\mu=6.22 \times 10^{11} \text{ dyne/cm}^2$.

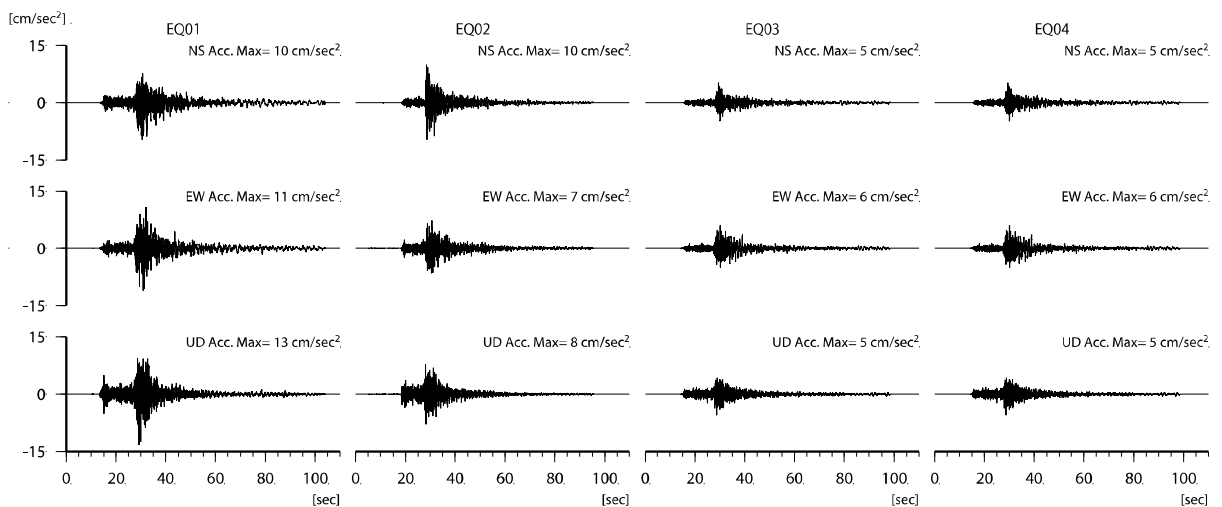
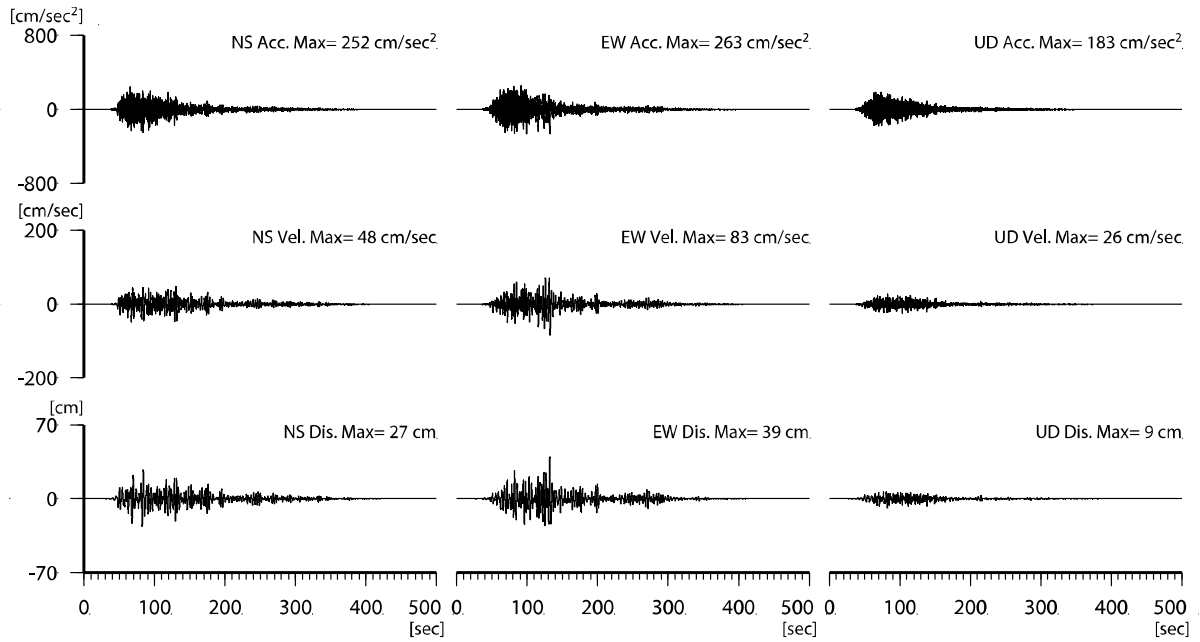
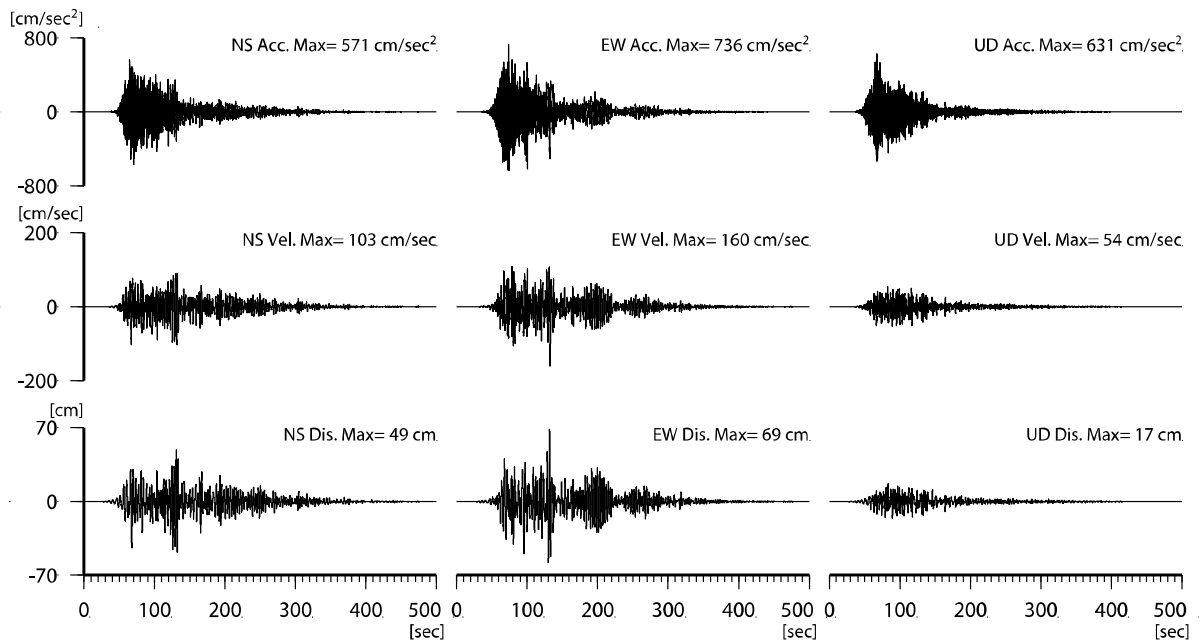


Figure 3.2. Observed waveforms of the small events used as the empirical Green's functions at NGY.



(a) Case 1



(b) Case 2

Figure 3.3. Synthetic waveforms at NGY.

synthetic waveforms. The seismic intensities of the 1854 Ansei-Tokai earthquake are estimated from the damage by Iida (1985). The JMA seismic intensities of the synthetic waveforms in Case 1 are comparable to those of the 1854 Ansei-Tokai earthquake, and the JMA seismic intensities of the synthetic waveforms in Case 2 are larger than those of the 1854 Ansei-Tokai earthquake.

4. CONCLUSIONS

We proposed a consistent source model both for the strong ground motions and tsunami of the huge subduction earthquake along the Nankai Trough. And we simulated the strong ground motions in and

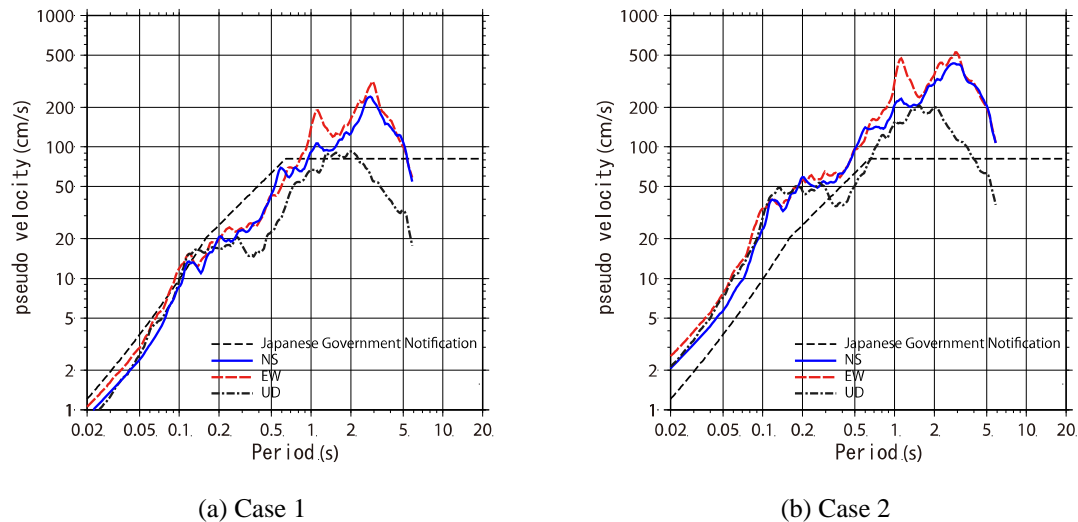


Figure 3.4. Pseudo velocity response spectra of the synthetic waveforms at NGY ($h=5\%$).

Table 3.2. Instrumental seismic intensities and JMA seismic intensities of the synthetic waves and the JMA seismic intensities in the 1854 Ansei-Tokai earthquake

	NGY		AICP12		SZO024		MIEP02	
Case 1	5.7	6-lower	6.5	7	5.8	6-lower	6.5	7
Case 2	6.4	6-upper	7.3	7	6.4	6-upper	7.3	7
The 1854 Ansei-Tokai earthquake*	6		6-7		6-7		6-7	

* Estimated from damage by Iida (1985).

around Aichi Prefecture using the empirical Green's functions based on the fault models including some asperities. In case that short-period level was assumed to be equal to the average for crustal earthquakes, the JMA seismic intensities of the synthetic waves were comparable to those of the 1854 Ansei-Tokai earthquake.

ACKNOWLEDGEMENTS

We appreciate National Research Institute for Earth Science and Disaster Prevention, Nagoya City, Aichi Prefecture, and Mie Prefecture for providing us with the strong motion data. We appreciate Japan Agency for Marine-earth Science and Technology for providing us with the crustal structure provided referred from the Special Project for Earthquake Disaster Mitigation in Urban Areas, and the Tokai-Tonankai-Nankai Earthquake Joint Project.

REFERENCES

- Central Disaster Management Council (2003). Conference document, 16th conference of the Special Board of Inquiry on Tonankai and Nankai earthquake, <http://www.bousai.go.jp/jishin/chubou/nankai/16/>. (in Japanese)
- Central Disaster Management Council (2012). <http://www.bousai.go.jp/chubou/suishinkaigi/4/>. (in Japanese)
- Dan, K., M. Watanabe, T. Sato, and T. Ishii (2001). Short-period source spectra inferred from variable-rupture models and modeling of earthquake faults for strong motion prediction, *Journal of Structural and Construction Engineering (Transactions of the Architectural Institute of Japan)*. **No.545**: pp.51-62. (in Japanese with English abstract)
- Eshelby, J. D. (1957). The determination of the elastic field of an ellipsoidal inclusion, and related problems, *Proceedings of the Royal Society of London. Series A*, **Vol. 241**: pp. 376-396.
- Iida, K. (1985). Investigation of Historical Earthquakes(6) : Earthquake and Tsunami Damages and Seismic Intensity Distribution by the Ansei Earthquake of December 23, 1854, *Bulletin of Aichi Institute of Technology*. **Part B, No.20**: pp. 167-182.
- Utsu, T. (2001). Seismology, 3rd edition, Kyoritsu (in Japanese).